

<sup>11</sup>Li, A., "Experimental and Numerical Study of Three-Dimensional Laminar Separated Flow Adjacent to Backward-Facing Step," Ph.D. Dissertation, Dept. of Mechanical and Aerospace Engineering and Engineering Mechanics, Univ. of Missouri, Rolla, MO, 2001.

## Generalized Nonequilibrium Binary Scaling for Shock Standoff on Hypersonic Blunt Bodies

George R. Inger\*

Iowa State University, Ames, Iowa 50011

and

Charlotte Higgins† and Richard Morgan‡

University of Queensland,

Brisbane, Queensland 4072, Australia

### Introduction

THE shock standoff distance  $\delta_s$  in a blunt-body stagnation region (Fig. 1) is sensitive to the thermochemistry within the shock layer<sup>1</sup> and, hence, an important observable in hypervelocity test facilities.<sup>2</sup> Although numerical codes are available to predict  $\delta_s$ , they are expensive for engineering parametric studies and do not yield physical insight and similitude laws needed for experimental design and data interpretation. On the other hand, existing analytical methods may not permit extension to include multitemperature ionization. The present paper examines a new analytical theory<sup>3</sup> of shock standoff with a nonequilibrium-dissociated shock layer to demonstrate a generalized binary scaling property for high-altitude hypervelocity flight simulation work.

### Theoretical Formulation

We consider a blunt nose region at zero angle of attack under the following assumptions (Fig. 1): 1) The postshock static pressure is a known constant across the shock layer. 2) The tangential velocity component is of the form  $U \approx \beta_s x$ , where  $\beta_s$  is an appropriately defined known constant equal to the effective stagnation point velocity gradient reflecting the  $U(y)$  variation. 3) Low Reynolds number viscous shock layer effects are negligible. For shock layer Reynolds numbers above 300 (pertaining to many applications), these assumptions are sufficient to model the main aerothermochemical aspects of the flow along the stagnation line  $x \rightarrow 0$ .

Regardless of the gas or its chemistry, continuity yields the normal velocity component  $V$  as

$$\rho(y)V(y) = -(1+J)\beta_s \int_0^y \rho \, dy \quad (1)$$

where  $J = 0, 1$  for two-dimensional or axisymmetric flow, respectively. When the density-stretched coordinate  $\eta$  is introduced,

$$\eta \equiv (1+J) \frac{\beta_s R_B}{U_\infty} \int_0^y \frac{\rho}{\rho_\infty} d\left(\frac{y}{R_B}\right) \quad (2)$$

Received 15 April 2002; revision received 28 June 2002; accepted for publication 28 June 2002. Copyright © 2002 by the American Institute of Aeronautics and Astronautics, Inc. All rights reserved. Copies of this paper may be made for personal or internal use, on condition that the copier pay the \$10.00 per-copy fee to the Copyright Clearance Center, Inc., 222 Rosewood Drive, Danvers, MA 01923; include the code 0887-8722/03 \$10.00 in correspondence with the CCC.

\*Professor, Department of Aerospace Engineering and Engineering Mechanics. Associate Fellow AIAA.

†Graduate Research Student, Centre for Hypersonics.

‡Professor, Centre for Hypersonics.

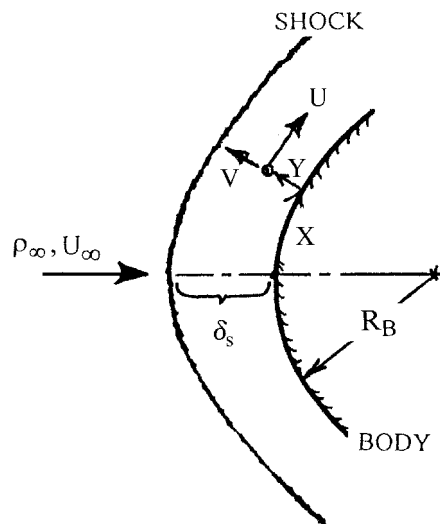


Fig. 1 Schematic of blunt-body stagnation shock layer.

Eq. (1) yields simply  $\rho V = -\rho_\infty U_\infty \eta$ . Because  $\rho V = -\rho_\infty U_\infty$  behind the shock,  $\eta = 1$  is, thus, the shock location regardless of the flow chemistry or dimensionality. The physical standoff distance  $\delta_s = (y)_{\eta=1}$  by Eq. (2) is then

$$\frac{\delta_s}{R_B} = \left( \frac{U_\infty}{\beta_s R_B} \right) \left( \int_0^1 \left( \frac{\rho_\infty}{\rho} \right) d\eta / (1+J) \right) \quad (3)$$

Equation (3) shows that once the density profile  $\rho(\eta)$  is found using the species, energy, and state equations, one integration yields  $\delta_s$  in a convenient nondimensional form.

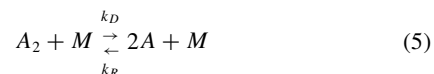
For dissociation involving the net formation of an atom mass fraction  $\alpha$ , we have along the stagnation line (neglecting diffusion) that  $\rho V \, d\alpha/dy = \dot{w}_\alpha$ , where  $\dot{w}_\alpha$  is the net chemical rate of atom mass formation per unit volume. Then applying Eq. (2), we obtain the nondimensional equation

$$\eta \frac{d\alpha}{d\eta} = \frac{-(\dot{w}_\alpha/\rho)}{(1+J)\beta_s} = \frac{-(R_B U_\infty)(\dot{w}_\alpha/\rho)}{(1+J)(\beta_s R_B/U_\infty)} \quad (4)$$

where both  $\dot{w}_\alpha/\rho$  and  $U_\infty/R_B$  have the same units of reciprocal time.

### Application to Dissociating Diatomic Gases

We now consider the specific case of a diatomic gas that undergoes the dissociation-recombination reaction



where  $M$  is a third body (molecule  $A_2$  or atom  $A$ ),  $k_D$  is the dissociation rate, and  $k_R$  is the recombination rate. The corresponding  $\dot{w}_\alpha$  is formulated from the law of mass action combined with the principle of detailed balancing and the use of the usual mole-mass fraction relationship, giving Eq. (4) as<sup>3</sup>

$$\eta \frac{d\alpha}{d\eta} = \frac{-k_{DA2} \rho_\infty R_B U_\infty}{2(1+J) R_u T \lambda} \sqrt{\frac{(1-\varepsilon_F)}{2\varepsilon_F}} \left\{ 1 + \left[ 2 \left( \frac{k_{DA}}{k_{DA2}} \right) - 1 \right] \alpha \right\} \times (1+\alpha)^{-1} \left\{ (1-\alpha) - \left( \frac{4\rho R_{A2} T}{K_{eq}} \right) \alpha^2 \right\} \quad (6)$$

where  $\varepsilon_F = \rho_\infty/\rho_F$ ,  $k_{DA2} \equiv CT^n e^{-T_D/T}$ ,  $c_j$  are mass fractions [ $c_A = \alpha$ ,  $c_{A2} = (1-\alpha)$ ], and  $K_{eq} = p_{ref}(T/T_{ref})^s e^{-(T_D/T)}$  in terms of the parameters  $p_{ref}$ ,  $T_{ref}$ ,  $s$ , and the dissociation temperature  $T_D$ .

The density  $\rho$  can be expressed in terms of  $\alpha$ , the pressure  $p$ , and the mixture temperature  $T$  by the equation of state, which on use of Dalton's law becomes

$$p = \rho(R_u/M_{A2})T(1+\alpha) \quad (7)$$

Here  $p \approx \rho_\infty U_\infty^2 (1 - \varepsilon_F)$  and  $\beta_S R_B / U_\infty \approx \sqrt{[2\varepsilon_F(1 - \varepsilon_F)]\lambda}$  from constant density shock layer Newtonian theory (see Ref. 4), where  $\lambda = k/\arcsin k$  with  $k = \sqrt{(1 - 3\varepsilon_F)/\sqrt{(3\varepsilon_F)}}$  for  $J = 0$  and  $\lambda = [1 + \sqrt{(8\varepsilon_F/3)}]/\sqrt{(8\varepsilon_F/3)}$  for  $J = 1$ . The corresponding energy conservation equation for steady, adiabatic, nonradiating shock layer (constant total enthalpy) at hypersonic flight conditions ( $U_\infty^2 \gg R_{A_2} T_\infty$ ) is<sup>3</sup>

$$\alpha + \frac{5}{2}(T/T_D) \left[ 1 + \alpha + \frac{2}{5}(1 - \alpha)(J_V + 1) \right] \approx (U_\infty^2/2h_D) + \alpha_\infty \quad (8)$$

where  $h_D \equiv R_{A_2} T_D = R_u T_D / M_{A_2}$ ,  $M_{A_2}$  is the molecular weight and  $J_V$  is an index that indicates the fraction of classical vibrational internal molecular energy assumed to be activated, for example,  $J_V = 1$  for complete activation,  $J_V = 0$  for negligible vibration, and  $J_V = \frac{1}{2}$  for the Lighthill ideal dissociating gas model.

### Similitude Properties and Binary Scaling

The foregoing indicates that the shock properties obey the following general similitude law for dissociating diatomic gases:  $\alpha(\eta), \theta(\eta), \ell(\eta) = f_{ns}[\Gamma_D, \tau_D, \alpha_\infty, (1 - \varepsilon_F)\rho_\infty/\rho_{ref}]$ , where  $\theta \equiv T/T_D$ ,  $\mathcal{I} \equiv \rho/\rho_\infty(1 - \varepsilon_F)$  and  $\tau_D \equiv U_\infty^2/2h_D$ . Here  $\rho_{ref} \equiv p_{ref} M_{A_2} (T_D/T_{ref})^s / R_u T_D$ , and  $\Gamma_D$  is the blunt nose Damköhler number

$$\Gamma_D \equiv \frac{C T_D^{N-1} R_B (1 - \varepsilon_F) \rho_\infty U_\infty}{2(1 + J) R_u \sqrt{2\varepsilon_F(1 - \varepsilon_F)} \lambda} \quad (9)$$

The corresponding scaling law governing  $\delta_s$ , from Eq. (3), is

$$(1 + J) \frac{\delta_s}{R_B} (1 - \varepsilon_F) \sqrt{2\varepsilon_F(1 - \varepsilon_F)} = \int_0^1 \ell^{-1}(\eta) d\eta \quad (10)$$

$$\equiv I \left[ \Gamma_D, \tau_D, \alpha_\infty, \frac{(1 - \varepsilon_F) \rho_\infty}{\rho_{ref}} \right]$$

when  $I$  is an integral function of the indicated scaling parameters and the last term on the right derives from the recombination term  $\sim \alpha^2$  in Eq. (6).

The practical utility of Eq. (10) obtains in those high-altitude/hypervelocity regimes of flight where recombination is negligible and the last parameter drops out. Then the appropriately nondimensionalized standoff distance depends for a given  $\alpha_\infty$  only on the Damköhler number  $\Gamma_D$  and the parameter  $\tau_D$ , regardless of altitude  $\rho_\infty$ , flight velocity, or body size. A particular version of this binary scaling for fixed  $U_\infty$  and  $\rho_\infty \cdot R_B$  has in fact been used for some time<sup>5,6</sup> to simulate nonequilibrium flows. A second and newer aspect, which we will discuss, deals with the roles of the parameters  $\alpha_\infty$  and (especially)  $\tau_D$ . In particular, we examine when  $\tau_D$  ceases to be influential and, hence, no longer restricts the usual binary scaling to require a fixed type of gas and/or flight velocity. Such a situation is important in hypervelocity testing because then the similitude requirements are unhooked from the need to duplicate  $\tau_D$  and, hence,  $U_\infty$ .

### Parametric Study Results

#### Damköhler Number Correlation

Based on the chemical kinetic data of Park<sup>7</sup> and the assumption that  $J_V = \frac{1}{2}$ , Fig. 2 shows the Damköhler number effect in terms of the nondimensional standoff distance ratio  $r_s \equiv (\delta_s - \delta_{s,eq})/(\delta_{s,F} - \delta_{s,eq})$ , where the subscripts eq and F denote equilibrium and frozen shock layer values, respectively. These results are plotted vs the modified Damköhler number  $\Omega$  (proportional to  $\Gamma_D$ ) defined by  $\Omega \equiv \theta_F^{N-1} e^{-1/\theta_F} (1 - \alpha_\infty) \Gamma_D [1 + [2(k_{DA}/k_{DA2}) - 1]\alpha_\infty]/(1 + \alpha_\infty)$ . When it is noted that  $r_s$  always lies between 0 in the equilibrium limit and unity in the opposite chemically frozen limit, this presentation efficiently collapses both theory and experiment to nearly universal sets of curves. Also shown is the envelope of combined experimental data/numerical computational fluid dynamic calculations.<sup>8-10</sup> It is seen that the present theory is in good agreement in predicting a significant decrease in  $r_s$  as  $\Omega$  increases from the chemically frozen limit ( $\Omega \rightarrow 0, r_s = 1$ )

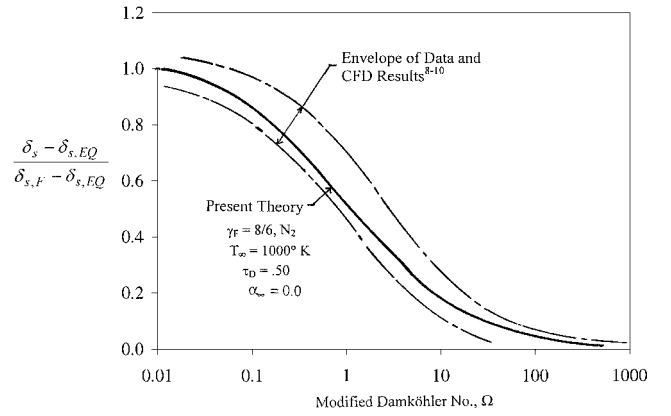


Fig. 2 Correlation of nondimensional shock standoff distance vs Damköhler number.

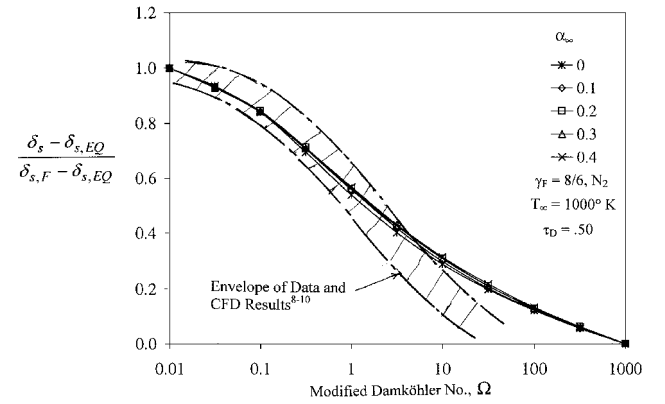


Fig. 3a Effect of freestream dissociation on the  $r_s(\Omega)$  correlation.

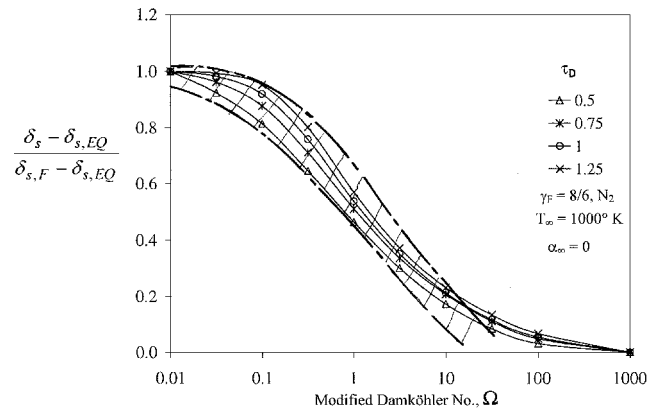


Fig. 3b Influence of the similitude parameter  $\tau_D$  on the  $r_s(\Omega)$  correlation.

to the equilibrium-dissociated limit ( $\Omega \rightarrow \infty, r_s = 0$ ). The various analyses lie within the experimental accuracy ( $\pm 10\%$ ) of the available data; indeed, the present theory lies near its center.

#### Freestream Dissociation Effect

The effect of nonequilibrium freestream dissociation  $\alpha_\infty$  on  $r_s$  over the entire nonequilibrium range is shown in Fig. 3a. For  $0 \leq \alpha_\infty \leq 0.4$ , it is seen that  $\alpha_\infty$  has a negligible effect up to  $\Omega \leq 100$ ; within the experimental uncertainty, the  $\alpha_\infty$ -effect has, thus, been almost completely accounted for in the  $\delta_{s,eq}$  and  $\delta_{s,F}$  values involved in  $r_s$  and its influence on  $\Omega$ .

#### Nondimensional Kinetic Energy Parameter $\tau_D$

The similitude parameter  $\tau_D$  represents the ratio of the flight kinetic energy to the dissociation energy of the gas; its influence on

the  $r_s$  vs  $\Omega$  variation is shown in Fig. 3b. For  $\tau_D \ll 1$ , it has a significant influence on  $r_s$  by decreasing the relative nonequilibrium effect with increasing  $\tau_D$ . However, when  $\tau_D \geq 1$ , the  $r_s$  vs  $\Omega$  correlation becomes insensitive to  $\tau_D$ . Indeed, for  $\tau_D \geq 1$ , its parametric effect is far smaller than the typical experimental data uncertainty, and, thus,  $\tau_D$  ceases to be relevant. In such cases, which embrace a wide range of planetary entry vehicle conditions, we, thus, obtain the generalized binary scaling that the ratio  $r_s$  depends only on  $\Omega$  regardless of the specific values of  $\rho_\infty$ ,  $R_B$ ,  $U_\infty$ , and  $\alpha_\infty$  or type of gas.

With regard to practical applications, the following simple closed-form expression has been found to fit the curve (Fig. 3) throughout the entire nonequilibrium regime:

$$r_s \approx \frac{6\sqrt{1 + 5.6\Omega} - 1}{5 + 20\Omega} \quad (11)$$

Equation (11) yields the linear function  $r_s \cong 1 - 0.70\Omega$  in the nearly frozen limit  $\Omega \ll 1$ , and the inverse square root  $r_s \cong 0.70\Omega^{-1/2}$  for nearly equilibrium flow  $\Omega \gg 1$ .

### Conclusion

We have presented some new parametric study results from a recent analytical theory of hypersonic blunt nose shocks standoff<sup>6</sup> which establish an extended nonequilibrium-dissociation binary scaling concept wherein the need to simulate flight velocity is eliminated when the parameter  $\tau_D \equiv U_\infty^2/2hD$  is greater than unity.

### Acknowledgments

This work was partially supported by the Australian Research Council and the University of Queensland travel scheme.

### References

- <sup>1</sup>Hornung, H. G., and Smith, G. H., "The Influence of Relaxation on Shock Detachment," *Journal of Fluid Mechanics*, Vol. 93, Pt. 2, 1979, pp. 225–239.
- <sup>2</sup>McIntyre, T. J., Wegener, M. J., Bishop, A. I., and Rubinsztein-Dunlop, H., "Simultaneous Two-Wavelength Holographic Interferometry in a Supersonic Expansion Tube Facility," *Applied Optics*, Vol. 36, No. 31, 1997, pp. 8128–8134.
- <sup>3</sup>Inger, G. R., Higgins, C., and Morgan, R., "Shock Standoff on Hypersonic Blunt Bodies in Nonequilibrium Gas Flows," *Journal of Thermophysics and Heat Transfer*, Vol. 16, No. 2, 2002, pp. 245–250.
- <sup>4</sup>Hayes, W. D., and Probstein, R. F., *Hypersonic Flow Theory*, Academic Press, New York, 1959, pp. 150–162.
- <sup>5</sup>Gibson, W., "Dissociation Scaling for Nonequilibrium Blunt Nose Flow," *ARS Journal*, Vol. 32, No. 4, 1962, pp. 285–287.
- <sup>6</sup>Stalker, R. J., "A Similarity Transformation for Blunt-Body Flows," AIAA Paper 86-0125, June 1986.
- <sup>7</sup>Park, C., "Assessment of Two-Temperature Kinetic Model for Dissociating and Weakly Ionizing Nitrogen," *Journal of Thermophysics and Heat Transfer*, Vol. 2, No. 1, 1988, pp. 8–16.
- <sup>8</sup>Freeman, N. C., "Non-Equilibrium Flow of an Ideal Dissociating Gas," *Journal of Fluid Mechanics*, Vol. 4, Pt. 3, 1958, pp. 407–425.
- <sup>9</sup>Hornung, H. G., "Non-Equilibrium Dissociating Nitrogen Flow Over Spheres and Circular Cylinders," *Journal of Fluid Mechanics*, Vol. 53, 1972, pp. 149–176.
- <sup>10</sup>Hornung, H. G., and Wen, C. Y., "Non-Equilibrium Dissociating Flow Over Spheres," *Journal of Fluid Mechanics*, Vol. 299, 1995, pp. 389–405.